Wind Generator Stability Enhancement by Using an Adaptive Artificial Neural Network-Controlled Superconducting Magnetic Energy Storage

Hany M. Hasanien, *Senior Member, IEEE,* S. Q. Ali, *Member, IEEE,* and S.M. Muyeen, *Senior Member, IEEE*

Abstract—**This paper presents a novel adaptive artificial neural network (ANN)-controlled superconducting magnetic energy storage (SMES) to enhance the transient stability of a grid-connected wind generator system. The control strategy of the SMES unit is developed based on cascaded control scheme of a voltage source converter and a two-quadrant DC-DC chopper using insulated gate bipolar transistors (IGBTs). The proposed controller is used to control the duty cycle of the DC-DC chopper. Detailed modeling and control strategies of the system are presented. The effectiveness of the proposed adaptive ANN-controlled SMES is then compared with that of a conventional proportional-integral (PI)-controlled SMES. The validity of the proposed system is verified with the simulation results which are performed using the standard dynamic power system simulator PSCAD/EMTDC.**

***Index Terms*—Adaptive artificial neural network controller, superconducting magnetic energy storage, voltage source converter, wind generator stability.**

I. INTRODUCTION

AS a result of shortage of the fossil fuel in generating electrical power from conventional power plants and the major interest in a clear environment, many efforts have been done to produce electrical energy from the renewable energy sources such as photovoltaic systems and wind energy conversion systems. The wind energy has continued its growth worldwide in these recent years. Over the past ten years, the global wind power capacity has continued to grow at an average cumulative rate of over 30%, and 2008 was another record year with more than 27 GW of new installations, bringing the total up to over 120 GW [1]. Because of these highly installations which increase day by day of wind turbines to the existing networks, many problems including transient stability of wind generators should be addressed, studied, and analyzed.

Currently, there are several types of energy storage devices in the market such as battery energy storage systems (BESS), energy capacitor systems (ECS), flywheel energy storage systems (FESS), and superconducting magnetic energy storage (SMES) systems. The BESS is the most commonly used but it has few demerits like limited life time, current and voltage restrictions, and environmental hazard [2]. Due to the development of power electronics, superconductivity, and computer science, the SMES system has received a great attention in the power systems applications. It has been utilized in distributed energy storage, spinning reserve, load following, automatic generation control, power quality improvement, reactive power flow control, voltage control, and transient stability enhancement [3]. The SMES has several merits include high storage efficiency which may reach 90 % or higher. Moreover, it has very fast response, where it can convert the power in the range of megawatts in several milliseconds [4]. Also, the number of charging and discharging cycles of SMES is not limited. However, the main demerit of the SMES system is its high cost, but it is expected to decrease in the near future with the development of power electronics, control strategies, and continuous research. Recently, the researches have been started to evaluate the SMES cost for electric power compensation [5].

The SMES is a large superconducting coil that can store electric energy in the magnetic field produced by the flow of a dc current through it. This coil is maintained at a specified low temperature by a cryogenic or dewar that contains helium or nitrogen liquid vessels. The real power and reactive power can be charged in or delivered from the coil of SMES according to the power system requirements. The interface between the power system and SMES coil is the power conditioning system (PCS) which has a very important role to demonstrate the validity of SMES in the dynamic control of the power system [3].

Several studies have been done to improve the stability of electric power systems with SMES [6]-[10]. In addition, a fuzzy logic-controlled SMES has been presented to improve the transient stability of a grid-connected synchronous generator system [11]. The results have been shown that the system responses using a fuzzy logic-controlled SMES are better than that obtained with a proportional-integral (PI)-controlled SMES. Furthermore, the coordination effect of a fuzzy logic-controlled SMES and optimal reclosing on the transient stability in a multi-machine power system during unsuccessful reclosing of circuit breakers has been investigated [12]. Although, the fuzzy logic systems incorporate an alternative way of thinking, it depends

Hany M. Hasanien and S. Q. Ali are with the Electrical Engineering Department, College of Engineering, King Saud University, 11421, Riyadh, S.A. (e-mail: hanyhasanien@ieee.org).

S. M. Muyeen is with the Electrical Engineering Department, The Petroleum Institute, Abu Dhabi, U.A.E.

mainly on the experience of the designer in tuning the membership functions.

There are several literature surveys related to the applications of SMES to improve the transient stability of wind generator systems [13-14]. In these reported works, the fuzzy logic system and PI controller were used to control the SMES unit. Although, the PI controller is the most commonly used in the industry due to its robustness and offering a wide stability margin, it suffers from the sensitivity to the parameter variations and nonlinearity of dynamic systems. Notably, till now, the application of different control strategies to SMES is limited. The control technologies can provide a much efficient SMES unit which in turn leads to improve the transient stability of the wind generator systems.

Therefore, this paper presents a novel adaptive artificial neural network (ANN)-controlled SMES in the purpose of enhancing the transient stability of a grid-connected wind generator system. The control strategy of the SMES unit depends on the well-known cascaded control scheme of a voltage source converter and a two-quadrant DC-DC chopper using insulated gate bipolar transistors (IGBTs). The proposed controller is used to control the duty cycle of the DC-DC chopper. Detailed modeling and control strategies of the system are presented. The effectiveness of the proposed adaptive ANN-controlled SMES is then compared with that of a PI-controlled SMES. The validity of the proposed system is verified with the simulation results which are performed using the standard dynamic power system simulator PSCAD/EMTDC.

II. Wind Turbine Modeling

The mathematical relation to the mechanical power extraction from the wind can be expressed as follows [15]:

$$P_w = 0.5\rho\pi R^2 V_w^3 C_P(\lambda,\beta) \quad (1)$$

where P_w is the extracted power from the wind, ρ is the air density [kg/m^3], R is the blade radius [m], V_w is the wind speed [m/s], and C_p is the power coefficient which is a function of tip speed ratio, λ, and blade pitch angle, β [deg.] [16]. In this paper, C_p can be written as follows [17]:

$$\lambda = \frac{V_w}{\omega_B}$$

$$C_P = \frac{1}{2}(\lambda - 0.022\beta^2 - 5.6)e^{-0.17\lambda} \quad (2)$$

where ω_B is the blade angular velocity [rad/s]. Fig. 1 shows the C_p-λ characteristics for different values of angle β. These characteristics represent the MOD-2 model.

III. Model System

The model system used in the wind generator stability enhancement is shown in Fig. 2. It consists of one synchronous generator (SG) and one wind turbine induction generator (IG). The aggregated wind turbine model is considered herein where many small size wind generators can be represented by a large capacity wind generator [18]. The wind generator feeds the power to an infinite bus through a transmission line with double circuit. A capacitor C is connected to the wind generator terminals for the purpose of compensating the reactive power at the steady state operation and its value has been selected to achieve unity power factor of the wind power station at the rated conditions. The parameters of SG and IG used in the simulation are shown in Table I. [13]. The SMES unit is connected to the wind generator terminal bus. The model of automatic voltage regulator and governor control system is shown in Fig. 3 and 4, respectively.

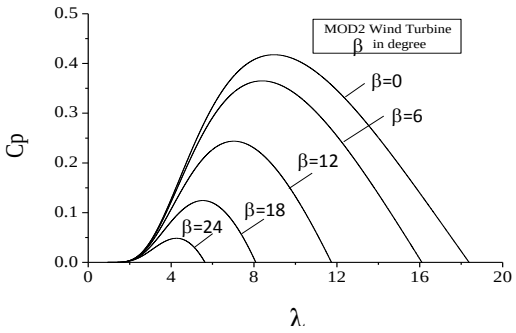

Fig. 1. C_P- λ characteristics for different pitch angles

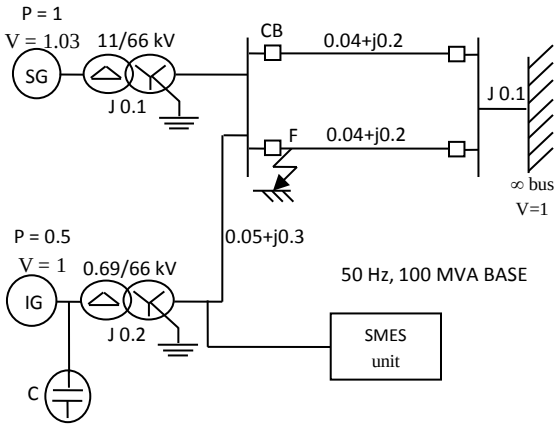

Fig. 2. Model System.

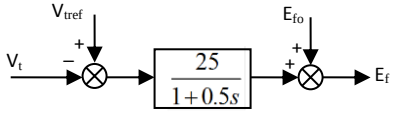

Fig. 3. Automatic voltage regulator model.

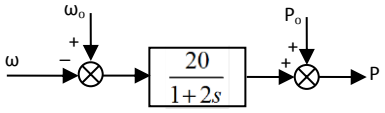

Fig. 4. Governor control system model.

IV. SMES Modeling and Control Scheme

The proposed model of SMES unit used in this paper, shown in Fig. 5, consists of a three-phase Wye-Delta 66/0.77 kV transformer, a six-pulse pulse width modulation (PWM) voltage source converter (VSC) using insulated gate bipolar transistors (IGBTs), a DC-link capacitor of 60 mF, a two-quadrant DC-DC chopper using IGBTs, and a superconducting coil of inductance 0.24 H. The stored energy, E [Joule], in a SMES system and its rated power, P [Watt], are described by the following equations:

$$E = \frac{1}{2} L_{sm} I_{sm}^2 \quad (3)$$

$$P = \frac{dE}{dt} = L_{sm} I_{sm} \frac{dI_{sm}}{dt} = V_{sm} I_{sm} \quad (4)$$

where L_{sm} is the inductance of the superconducting coil, I_{sm} is the dc current flowing through the coil, and V_{sm} is the

instantaneous voltage across the coil. The rated values of *E* and *P* for a SMES system under study are 0.05 MWH and 50 MW, respectively [19].

Table I
GENERATORS PARAMETERS

SG		IG	
MVA	100	MVA	50
r_a [pu]	0.003	r_1 [pu]	0.01
x_a [pu]	0.13	x_1 [pu]	0.18
x_d [pu]	1.2	x_{mu} [pu]	10
x_q [pu]	0.7	r_2 [pu]	0.015
x'_d [pu]	0.3	x_2 [pu]	0.12
x'_q [pu]	0.22	H [s]	1.5
x''_d [pu]	0.22		
x''_q [pu]	0.25		
T'_{do} [s]	5		
T''_{do} [s]	0.04		
T''_{qo} [s]	0.05		
H [s]	2.5		

A. VSC

The VSC is a three-phase rectifier/inverter that connects the superconducting coil with the ac power system. The well-known cascaded control scheme is considered in this study, as shown in Fig. 6. The dq quantities and three-phase electrical quantities are related to each other by the reference frame transformation. The angle of the transformation is detected from three-phase voltages (v_a,v_b,v_c) at the high voltage side of the transformer using Phase-Locked Loop (PLL). The difference between the reference dc-link voltage $V_{dc\text{-}ref}$ and the actual dc-link voltage V_{dc} is the dc-link voltage error, which is the input of a (PI-1) controller to produce the reference signal $I_{d\text{-}ref}$. Additionally, the difference between the reference induction generator voltage $V_{IG\text{-}ref}$ and its actual value V_{IG} represents the IG voltage error, which is the input of PI-1 controller to produce the reference signal $I_{q\text{-}ref}$. Moreover, both of the difference between I_d and $I_{d\text{-}ref,}$ and I_q and $I_{q\text{-}ref}$, follows a PI-2 to obtain the reference signals $V_{d\text{-}ref}$ and $V_{q\text{-}ref}$, respectively. These signals are converted to a three-phase sinusoidal reference waveform $V_{a,b,c\text{-}ref}$, which is compared with a triangular carrier waveform for generating the gate signals of IGBTs. The chosen frequency of the triangular carrier waveform is 1050 Hz. Fine tuning of the PI controller parameters is performed by trial and error, which is the most commonly used method to achieve the best system performance. The V_{dc} is kept constant at 1 kV through the simulation using the PWM VSC.

B. DC-DC Chopper

The energy of superconducting coil is stored or delivered by controlling the dc voltage across the coil using a two-quadrant DC-DC chopper. This dc voltage is controlled by the duty cycle of the chopper. When the duty cycle is greater or lower than 50 %, the dc voltage is positive or negative and the coil is charged or discharged, respectively. In addition, at 50 % duty cycle, the net dc voltage across the coil is zero, which means that the coil is neither charged nor discharged. Fig. 7 shows the duty cycle control of the chopper. The difference between the induction generator real power P_{IG} and its reference $P_{IG\text{-}ref}$ represents the power error, which is the input of a PI-3 controller. The output of PI-3 controller is used to update the duty cycle signal (D). The PWM reference signal is compared with a triangular carrier waveform to generate the gate signals for the IGBTs of the DC-DC chopper. The chosen frequency of the triangular waveform is 100 Hz.

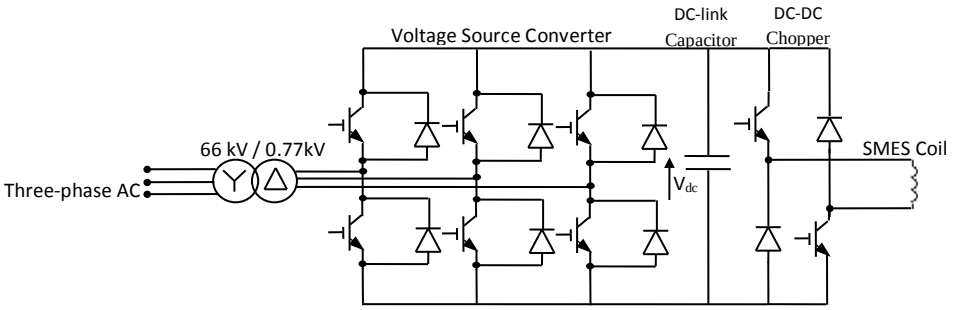

Fig. 5. Proposed SMES model.

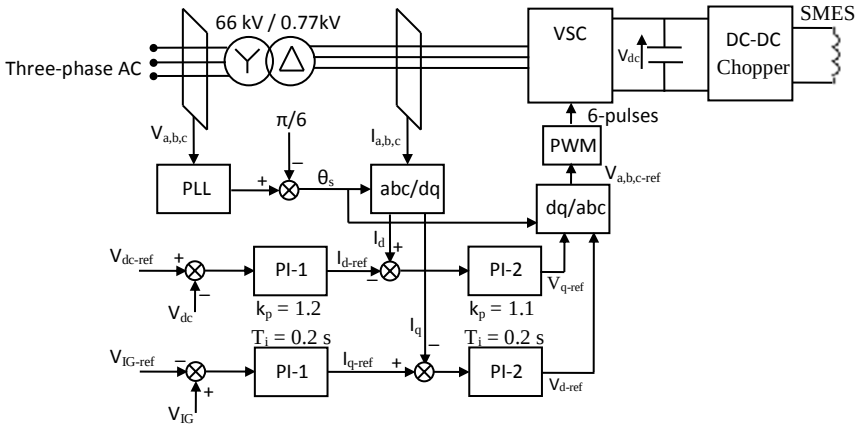

Fig. 6. Control block diagram of the VSC

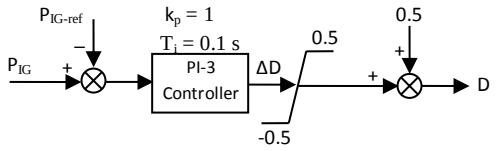

Fig. 7. Duty cycle control of the chopper.

V. Adaptive ANN Controller

A. Description of ANN

ANN controllers are computational models based on an analogy with biological neural networks. Biological neural networks can learn from experience and it follows that many ANN models can also learn. Usually, an ANN consists of a highly parallel ensemble of simple computing elements, or neurons. Furthermore, neurons usually have many interconnections with other neurons in the ANN. One class of ANN interconnection strategies is the feedforward strategy, which is used in this study. Relevant ANN model design considerations are the selection of inputs, the number of hidden layers, the number of neurons in each hidden layer and tuning the weights of the ANN.

The input vector of the ANN controller consists of the reference induction generator real power $P_{IG\text{-}ref}$, actual induction generator real power $P_{IG}(t)$, and the previous output signal from the ANN controller u(t-1). The inputs of the ANN controller have to be carefully chosen, as this dictates the boundness and stability of the desired trajectories. The selection of the number of hidden layers and the number of neurons in each hidden layer is performed by trial and error, which is the most commonly used method in ANN architecture design. A three layer feedforward neural structure with three neurons in one hidden layer is found to be a good balance between estimation error and ANN complexity. An ANN structure with a 3 × 3 × 1 structure (three neurons in input layer, three neurons in the hidden layer, and one neuron in output layer) is shown in Fig. 8. The number of input nodes is equal to the number of input signals, and the number of output node equals the number of output signals.

The output of a single neuron can be represented by the following equation:

$$a_i = f_i\left(\sum_{j=1}^{n} w_{ij}\, x_j(t) + b_i\right) \tag{5}$$

where f_i is the activation function, w_{ij} is the weighting factor, x_j is the input signal, and b_i is the bias. The most commonly used activation functions are nonlinear continuously varying types between two asymptotic values, namely, -1 and +1. Such functions are known as tansigmoid functions. The activation function used is the tansigmoid function in both the hidden and output layers.

B. Learning Algorithm

The adaptive ANN controller is based on the Widrow-Hoff adaptation algorithm. The Widrow-Hoff delta rule can be used to adapt the Adaline's weight vector [20]. The weight update equation for the original form of the algorithm can be written as:

$$W(t+1) = W(t) + \alpha \frac{e_p(t).x(t)}{|x(t)|^2} \tag{6}$$

where *W(t+1)* is the next value of the weight vector, *W(t)* is the present value of the weight vector, and *x(t)* is the present input vector. The present power error $e_p(t)$ is defined to be the difference between $P_{IG\text{-}ref}$ and P_{IG} (t).

Changing the weights yields a corresponding change in the error:

$$\Delta e_p(t) = \Delta(P_{IG-ref} - P_{IG}(t)) = -x^T(t)\Delta W(t) \tag{7}$$

In accordance with the Widrow-Hoff delta rule of Eq. (6), the weight change is as follows:

$$\Delta W(t) = W(t+1) - W(t) = \alpha \frac{e_p(t).x(t)}{|x(t)|^2} \tag{8}$$

Combining Equations (7) and (8) we obtain

$$\Delta e_p(t) = -\alpha \frac{e_p(t).x^T(t).x(t)}{|x(t)|^2} = -\alpha.e_p(t) \tag{9}$$

Therefore, the error is reduced by a factor of α as the weights are changed while holding the input pattern fixed. Presenting a new input pattern starts the next adaptation cycle. The next error is then reduced by a factor of α, and the process continues. The initial weight vector is usually chosen to be zero and is adapted until convergence.

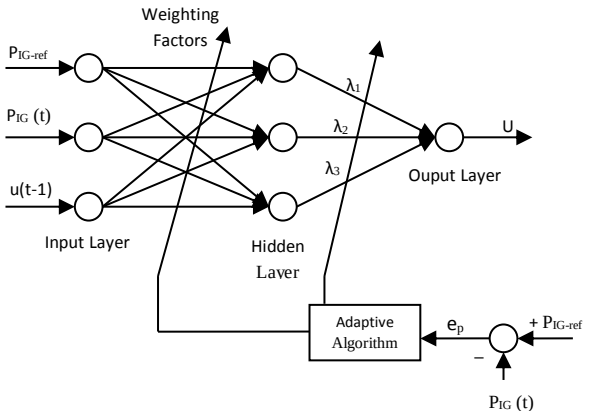

Fig. 8. ANN structure.

The output signal of the adaptive ANN controller u(t) after being rescaled is used to generate the duty cycle according to the following equation [21]-[23]:

$$D_{new} = D_{initial} - k.u \tag{10}$$

where $D_{initial}$ is the one step time delayed duty cycle signal, and *k* is a multiplying constant.

Thus, the proposed algorithm corrects errors and minimizes the mean square error between $P_{IG\text{-}ref}$ and $P_{IG}(t)$ over all times. The algorithm is best known for this property.

VI. Simulation Results

Detailed modeling and control strategies of the system under study are presented. Time domain simulation has been done using the standard dynamic power system simulator PSCAD/EMTDC [24]. The simulation time and time step are chosen 5 s and 10 μs, respectively. The

wind speed is fixed at the rated value of 11.8 m/s. For the transient stability study, a severe symmetrical three-line to ground fault (3LG) is considered as the network disturbance. The fault occurs at 0.1 s at fault point F, as shown in Fig. 2. The circuit breakers (CBs) on the faulted line are opened at 0.2 s, and at 1.0 s the CBs are reclosed. It is assumed that the reclosure of CBs are successful. The real power and reactive power can be charged in or delivered from the coil of SMES during the network disturbance. Therefore, the IG terminal voltage can return back at its prefault level, as shown in Fig. 9 (a). It can be realized that the IG terminal voltage response when an adaptive ANN-controlled SMES is used, is a better damped response than that obtained when a PI-controlled SMES is considered. Figs. 9 (b) and (c) show the IG real and reactive power responses, respectively. Notably, the IG real and reactive power can maintain at the prefault value using both of adaptive ANN-controlled SMES and PI-controlled SMES but adaptive ANN-controlled SMES contributes to a better damped response. In addition, the IG speed is unstable without using the SMES unit and stable with adaptive ANN-controlled SMES or PI-controlled SMES, as shown in Fig. 9 (d). Fig. 9 (e) shows the SG terminal voltage response which is smoothed when adaptive ANN-controlled SMES is used than that of a PI-controlled SMES. The SG real and reactive power responses are shown in Fig. 9 (f) and (g), respectively. Fig. 9 (h) shows the SG load angle response which expresses in the more transiently stable system when adaptive ANN-controlled SMES is used. The real power of adaptive ANN-controlled SMES is shown in Fig. 9 (i). The results prove that the wind turbine IG system and the SG system become stable using both of adaptive ANN-controlled SMES and PI-controlled SMES. However, all the system responses using adaptive ANN-controlled SMES are better than that of using PI-controlled SMES. Therefore, adaptive ANN-controlled SMES is considered to be an effective means of enhancing the transient stability of the wind turbine IG systems.

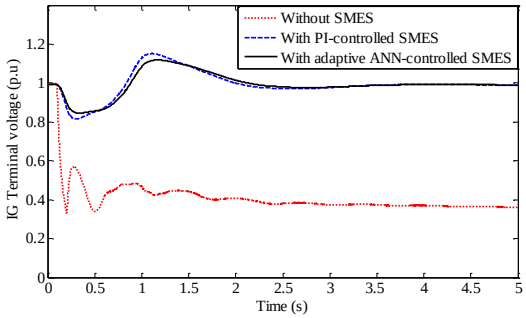

(a)

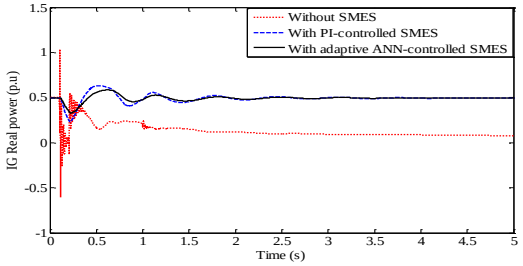

(b)

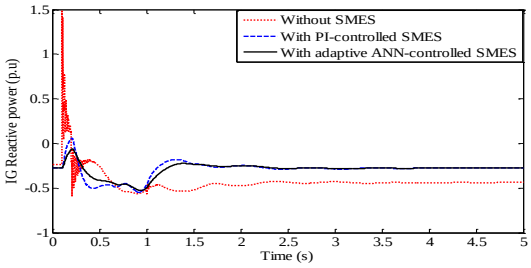

(c)

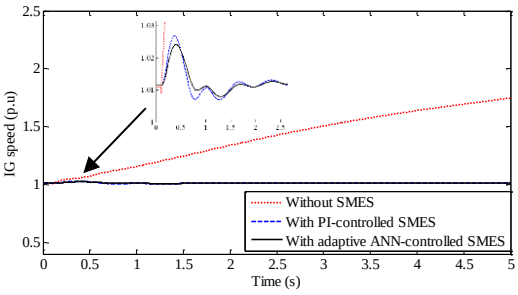

(d)

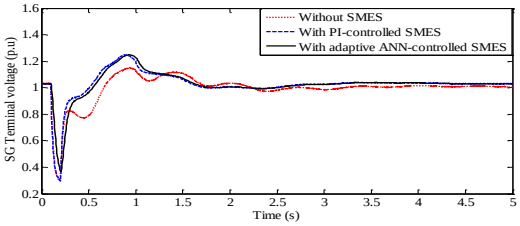

(e)

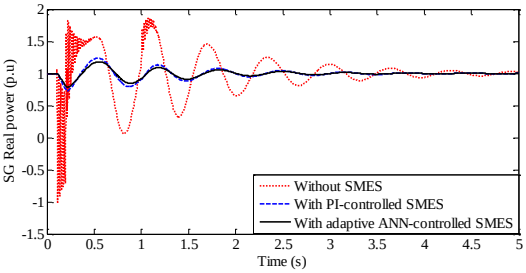

(f)

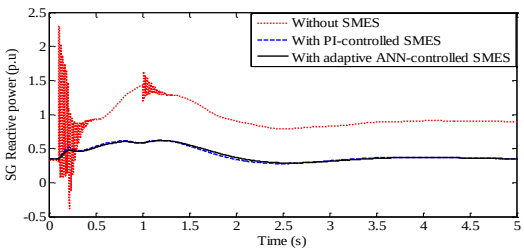

(g)

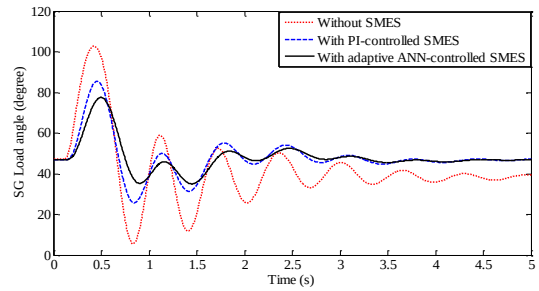

(h)

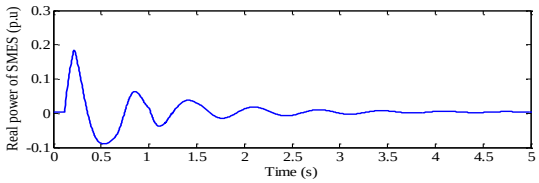

(i)

Fig. 9. Responses for 3LG fault. (a) IG terminal voltage. (b) IG real power. (c) IG reactive power. (d) IG speed. (e) SG terminal voltage. (f) SG real power. (g) SG reactive power. (h) SG load angle. (i) The real power of adaptive ANN-controlled SMES.

VII. Conclusion

This paper has introduced a novel adaptive artificial neural network-controlled SMES to enhance the transient stability of a grid-connected wind generator system. Detailed modeling and control strategies of the system under study are presented. The results have been shown that the integration of a PI or an adaptive ANN-controlled SMES with the wind generator system results in obtaining a stable system when it is subjected to a severe disturbance. The dynamic response of the system with adaptive ANN-controlled SMES is much better than that obtained with PI-controlled SMES. Adaptive ANN-controlled SMES was found to be an effective means for enhancing the stabilization of the wind generator system.

Acknowledgment

This project is fully funded by the Sustainable Energy Technologies Program, King Saud University.

References

[1] Global Wind Energy Council (GWEC), "Wind is a global power source," Global Trend-GWEC, online: http://www.gwec.net.

[2] Mohd. Hasan Ali, Bin Wu, and Roger A. Dougal, "An overview of SMES applications in power and energy systems," *IEEE Transactions on Sustainable Energy*, vol. 1, no. 1, pp. 38-47, April 2010.

[3] Marcelo Gustavo Molina, and Pedro Enrique Mercado, "Power flow stabilization and control of microgrid with wind generation by superconducting magnetic energy storage," *IEEE Transactions on Power Electronics*, vol. 26, no. 3, pp. 910-922, March 2011.

[4] IEEE Task Force on Benchmark Models for Digital Simulation of FACTS and Custom-Power Controllers, T&D Committee, "Detailed modeling of superconducting magnetic energy storage (SMES) system," *IEEE Transactions on Power Delivery*, vol. 21, no. 2, pp. 699-710, April 2006.

[5] Shinichi Nomura, Takakazu Shintomi, Shirabe Akita, Tanzo Nitta, Ryuichi Shimada, and Shinichiro Meguro, "Technical and cost evaluation on SMES for electric power compensation," *IEEE Transactions on Applied Superconductivity*, vol. 20, no. 3, pp. 1373-1378, June 2010.

[6] S.C. Tripathy, M. Kalantar, and R. Balasubramanian, "Dynamics and stability of wind and diesel turbine generators with superconducting magnetic energy storage unit on an isolated power system," *IEEE Transactions on Energy Conversion*, vol. 6, no. 4, pp. 579-585, December 1991.

[7] Y. Mitani, and K. Tsuji, "Power system stabilization by superconducting magnetic energy storage connected to rotating exciter," *IEEE Transactions on Applied Superconductivity*, vol. 3, no. 1, pp. 219-222, March 1993.

[8] Yoke Lin Tan, and Youyi Wang, "Augmentation of transient stability using a superconducting coil and adaptive nonlinear control," *IEEE Transactions on Power Systems*, vol. 13, no. 2, pp. 361-366, May 1998.

[9] Cheng-Ting Hsu, "Enhancement of transient stability of an industrial cogeneration system with superconducting magnetic energy storage unit," *IEEE Transactions on Energy Conversion*, vol. 17, no. 4, pp. 445-452, December 2002.

[10] A. Abu-Siada, and Syed Islam, "Application of SMES unit in improving the performance of an AC/DC power system," *IEEE Transactions on Sustainable Energy*, vol. 2, no. 2, pp. 109-121, April 2011.

[11] Mohd. Hasan Ali, T. Murata, and J. Tamura, "A fuzzy logic-controlled superconducting magnetic energy storage for transient stability augmentation," *IEEE Transactions on Control Systems Technology*, vol. 15, no. 1, pp. 144-150, January 2007.

[12] Mohd. Hasan Ali, T. Murata, and J. Tamura, "Transient stability enhancement by fuzzy logic-controlled SMES considering coordination with optimal reclosing of circuit breakers," *IEEE Transactions on Power Systems*, vol. 23, no. 2, pp. 631-640, May 2008.

[13] Mohd. Hasan Ali, Minwon Park, In-Keun Yu, Toshiaki Murata, and Junji Tamura, "Improvement of wind generator stability by fuzzy logic-controlled SMES," *IEEE Transactions on Industry Applications*, vol. 45, no. 3, pp. 1045-1051, May/June 2009.

[14] Li Wang, Shiang-Shong Chen, Wei-Jen Lee, and Zhe Chen, "Dynamic stability Enhancement and power flow control of a hybrid wind and marine-current farm using SMES," *IEEE Transactions on Energy Conversion*, vol. 24, no. 3, pp. 626-639, September 2009.

[15] S. Heier, "Grid Integration of Wind Energy Conversion System," Chicester, U.K., John Wiley & Sons Ltd., 1998.

[16] Hany M. Hasanien, and S. M. Muyeen, "Design Optimization of Controller Parameters used in Variable Speed Wind Energy Conversion System by Genetic Algorithms", *IEEE Transactions on Sustainable Energy*, vol. 3, no. 2, pp. 200-208, April 2012.

[17] P. M. Anderson and A. Bose, "Stability Simulation of Wind Turbine Systems," *IEEE Transactions on Power Apparatus and Systems*, vol. PAS-102, no.12, pp.3791-3795, December 1983.

[18] S. M. Muyeen, J. Tamura, and T. Murata, Stability Augmentation of a Grid-connected Wind Farm, Springer-VerlagLondon, ISBN 978-1-84800-315-6, October 2008.

[19] M.R.I. Sheikh, S.M. Muyeen, RionTakahashi, Toshiaki Murata and Junji Tamura, "Transient Stability Enhancement of Wind Generator Using Superconducting Magnetic Energy Storage Unit," CD Record of XVIII International Conference on Electrical Machines (ICEM 2008), Ref. No.1027, Portugal, Sep 6-9, 2008.

[20] B. Widrow and M. A. Lehr, "30 years of adaptive neural networks: Perceptron, madaline, and backpropagation," in *Proc. IEEE*, vol. 78, pp. 1415-1442, Sept. 1990.

[21] Hany M. Hasanien, "FPGA implementation of adaptive ANN controller for speed regulation of permanent magnet stepper motor drives," Energy Conversion and Management, vol. 52, issue 2, pp. 1252-1257, Feb. 2011.

[22] Hany M. Hasanien, and S. M. Muyeen, "Speed control of grid-connected switched reluctance generator driven by variable speed wind turbine using adaptive neural network controller", *Electric Power Systems Research, Elsevier*, vol. 84, no. 1, pp. 206-213, March 2012.

[23] Syed Q. Ali and Hany M. Hasanien, "Frequency Control of Isolated Network with Wind and Diesel Generators by Using Adaptive Artificial Neural Network Controller", *International Review of Automatic Control,Praise Worthy Prize*, vol.5, no.2, March 2012

[24] PSCAD/EMTDC Manual, Manitoba HVDC Research Center, 1994.